https://doi.org/10.48048/tis.2023.3530

Effect of Intensity and Wavelength of Illumination on the Photoelectronic Properties of Nanocrystalline CdSe Thin Films

Kangkan Sarmh[1,*] and Kamala Kanta Borah[2]

[1]*Department of Physics, Mangaldai Collge, Assam 784125, India*
[2]*Department of Chemistry, Mangaldai Collge, Assam 784125, India*

([*]Corresponding author's e-mail: ks.mcphys@gmail.com)

Received: 2 April 2022, Revised: 11 June 2022, Accepted: 18 June 2022, Published: 20 November 2022

Abstract

Photoelectronic properties of nanocrystalline CdSethin films prepared by chemical bath deposition (CBD) technique at room temperature are studied taking its molar concentration as a function. Structural analysis of the deposited thin films shows that change of molarity brings a variation in the crystalline sizes of the thin films. Such thin films show suitable photoelectronic properties for the construction of different optoelectronic devices. The photocurrents are observed to be significantly defect controlled in the visible range of wavelengths. The transport mechanism for the thin films is generally a doubly activated process and the photocurrent decay characteristics curves are found to exhibit 2 different decay times which actually correspond to 2 distinct trap levels.

Keywords: Decay time, Molarity, Nanocrystalline CdSe thin films, Photocurrent, Trap level

Introduction

In recent past much importance has been given in the field of II-VI group of materials because of their attractive photoelectronic properties and applications. CdSe is a compound semiconductor and is regarded as a prominent member of this group because of its very effective photo response behaviour [1-4]. It is being widely used as core material in different optoelectronic devices such as power efficient solar cells [5], sensors [6], thin film transistors [7], light emitting diodes [8] etc. Nanocrystalline thin films of CdSe have been prepared using different methods [9-16], out of which CBD technique is mainly used because of its simplicity, effectiveness and variability [17-19]. Although wide range of works on the synthesis and characterization of nanocrystalline thin films of CdSe have already been reported [9-19], but only few works on the photoelectronic properties specifically based on the wavelength and the intensity of incident illumination have been found in the available literatures [20,21]. Reported works have basically considered the complete range of visible light spectrum i.e. the white light illumination for photoconductive studies. But it is observed that photoelectronic properties of chemically deposited nanocrystalline CdSe thin films are governed not only by the deposition parameters like the molarity of the solution, rate of stirring, deposition temperature etc but also by wavelength and intensity of incident illumination. Deposition parameters in turn determine the structural aspects of the thin films whereas variations in the wavelength and intensity of incident illuminations bring significant changes in the various photoelectronic properties of the same film. Study of such properties of nanocrystalline thin films are essential requirements for proper application in different optoelectronic devices. Keeping these aspects in mind, in this work nanocrystalline CdSe thin films are prepared by CBD method at room temperature for different molarities (m) whose structural analysis are done and then some of the prominent photoelectronic properties of one of such representative thin films, illuminated by different monochromatic light of various intensities, are being reported in this paper whereas the same study was being reported for thermally deposited polycrystalline CdSe thin films in an earlier commutation [22].

Materials and methods

Preparation of nanocrystalline CdSe thin films

CdSe thin films were deposited on chemically and ultrasonically cleaned glass substrates by CBD method using solution of cadmium acetate, liquor ammonia and freshly prepared sodium selenosulphate (Na_2SeSO_3) solution. Na_2SeSO_3 solution was prepared by mixing selenium powder with anhydrous sodium sulphite in double distilled water using a refluxing unit. Cadmium acetate solutions of molarities 0.25, 0.50, 0.75 and 1M were taken as molar solutions in separate deposition baths at room temperature. To each solution 25 % ammonia solution was added drop by drop to optimize pH value under continuous gentle stirring at room temperature for 10 min till the solution became clear and transparent. The pH was maintained at around 10. To each such bath solution, freshly prepared Na_2SeSO_3 solution was added with continuous stirring. The colourless bath turned orange red within 1 h. The cleaned glass substrates were kept vertically in the chemical bath for 12 h for deposition using specially designed sample holder. Thus thin films were allowed to deposit on both surface of the substrates [23,24]. They were thoroughly washed with doubly distilled water and the set of thin films were then annealed in air for half an hour at 100 °C (**Figure 1**). The thickness (t) of the thin films was measured by multiple beam interferometer technique [25].

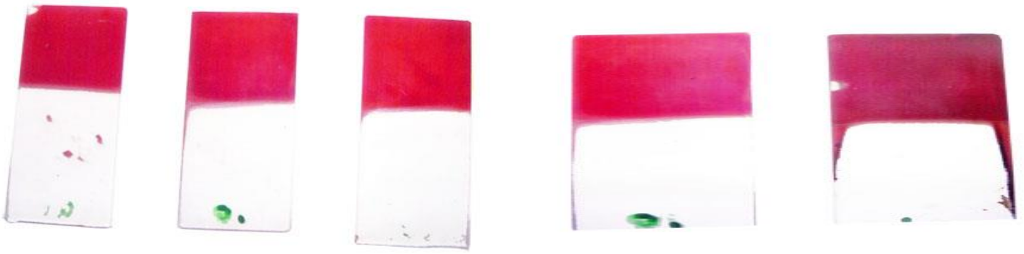

(a) (b)

Figure 1 Nanocrystalline CdSe thin films prepared by CBD method (a) 3 unannealed thin films of m= 1 M, t = 240 nm and (b) 2 unannealed (left one) and annealed (right one) thin films of m= 1 M, t = 290 nm

Characterization of nanocrystalline CdSe thin films

X-ray diffractogram (XRD) of CdSe thin films were taken by using Philips X-ray diffractometer (Philips X'Pert Pro) with CuKα radiations of wavelength 1.54Å. The diffractrometer was operated at 40 keV and 30 mA. An ECIL electrometer amplifier (EA815) of input impedance of $10^{14}\Omega$ (and higher) was used to measure dark and photocurrents. To provide bias, a series of highly stable dry cells of emf 9 volt each were used. The sample was kept suspended by thin enamelled copper wires inside a continuously evacuated glass jacket at room temperature. The entire experimental set up including the observer was housed in a suitably fabricated Faraday cage in order to avoid pick up noises. A set of C-Z metal interference filters of different wavelengths starting from 600 to 950 nm was used to obtain the monochromatic radiations (**Figure 2**). Light intensities were measured by using a highly sensitive APLAB luxmeter.

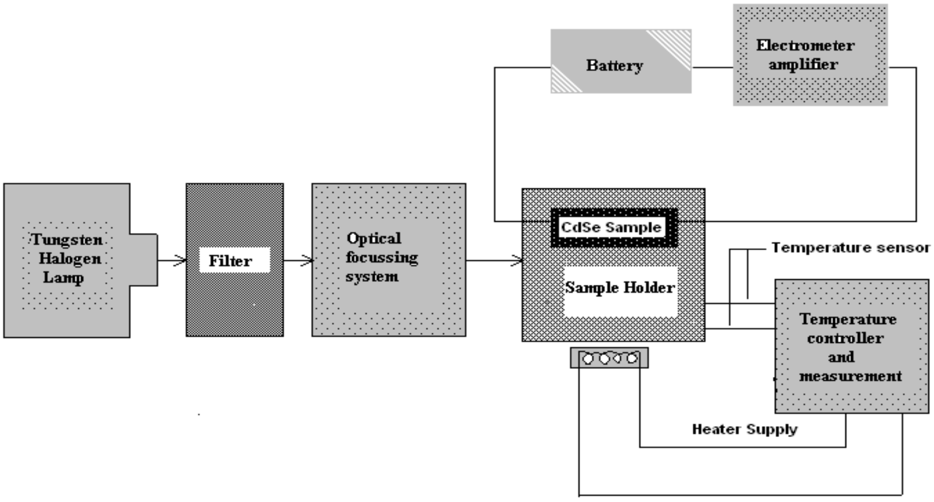

Figure 2 Block diagram of the experimental set up used for optoelectronic measurements.

Results and discussions

Structural studies

From the XRD of typical CdSe thin films (**Figure 3**) the diffraction peaks may be indexed to diffraction from the (111) and (220) planes of zincblende structure of CdSe. The lattice constant ‘a’ is found to be in between 5.642 and 5.844 Å. This is nearly in agreement with a_0 = 6.077 Å, the standard data obtained from JCPDS [26]. It is observed that value of ‘a’ is less than its bulk value 6.08 Å, which shows that the experimental thin films are under some strain. With increase of molarity, the full width at half maximum (FWHM) as obtained from these diffractograms are found to decrease indicating there by that due to an increase in average crystallite size, which are obtained in the range of 18 to 36 nm (calculated from XRD patterns), and decrease in strain, there is also a decrease in lattice imperfections. Larger numbers of Cd^{2+} and Se^{2-}ions react to form the deposit with increase of molarities of the solutions which results in the increase of crystallite size. With increase of molarity, the calculated values of dislocation densities (not presented here) are also found to decrease which indicates that at relatively higher molarities there occurs the formation of good quality thin films [23].

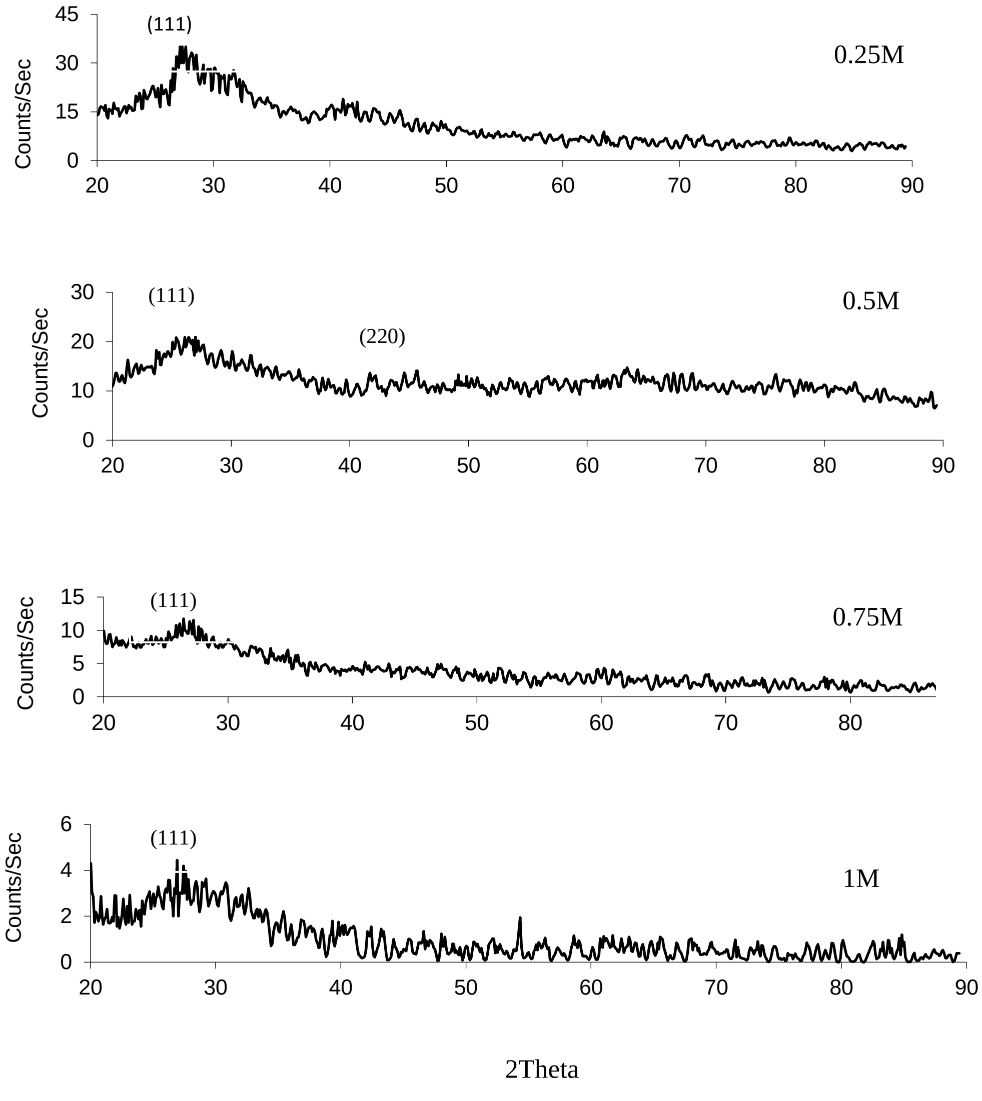

Figure 3 XRD patterns of 3 typical nanocrystalline CdSe thin films of t = 240 nm and of different m = 0.25, 0.5, 0.75 and 1.0M at room temperature.

Optoelectronic studies

I-V Characteristics

Variation of dark current, I_D with applied bias voltage for nanocrystalline thin films are found to be linear (ohmic) within the applied bias range [(-108 V)-0-(+108V)]. Let F is the field corresponding to this applied bias. For the low bias voltages of both polarities, current under illumination I_L varies linearly with bias and in high voltage range I_L increases nonlinearly with the applied bias. Here the difference of I_L and I_D is known as the photocurrent I_{ph} and considering the area of the film, the photocurrent density J_{ph} has been determined. When ln J_{ph} is plotted against $F^{½}$ the plots (**Figures 4**) are found to be linear in the high field regions and non-linear in low fields.

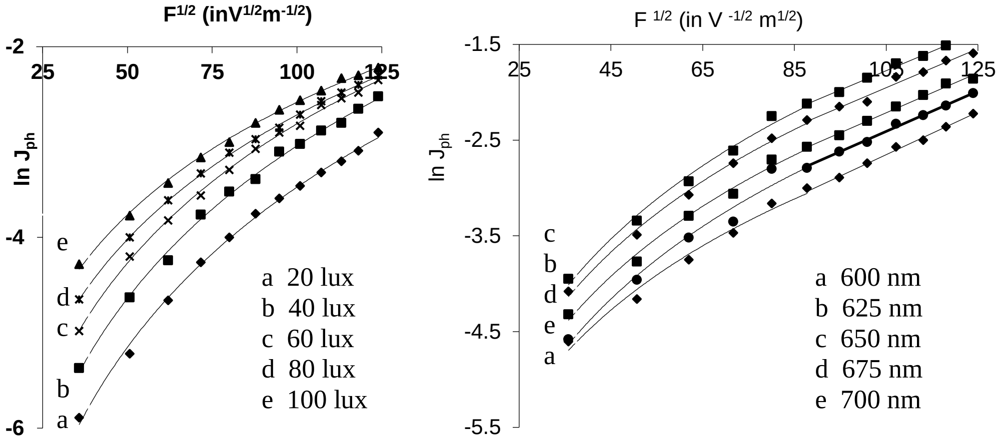

(a) (b)

Figure 4 ln J_{ph} vs $F^{1/2}$ plot for a CdSe thin (t=240 nm, m=1M) film (a) under monochromatic illuminations of 650 nm of different intensities (b) under different monochromatic illuminations of constant intensity.

It is apparent from the ln J_{ph} vs $F^{1/2}$ characteristics that, the basic nature of the curves under monochromatic illuminations are similar apart from the numerical values, both in low and the high field regions. This clearly shows that in high field region the conduction mechanism is of Poole-Frenkel type. This type of conductivity mainly depends upon the grain boundary potential barriers, which may be modified by the assistance of externally applied fields. The current density due to such type of conduction mechanism is given by [27];

$$J_{PF}=J_o\exp(\beta_{PF}F^{1/2}/kT) \quad (1)$$

where $\sigma_oF=J_o$ is the low field current density, β_{PF} is the Poole-Frenkel coefficient and other symbols have their usual significance. From the slops of ln J_{PF} vs $F^{1/2}$ plots the Poole-Frenkel coefficients are calculated which are found to be in the range $(5.4–5.9)\times10^{-4}$ eV $V^{-1/2}$ $m^{1/2}$.

Intensity dependence of photocurrent

The basic nature of intensity (ϕ) dependence of photocurrent for the CdSe thin films is found to follow the relation;

$$I_{ph} = C\phi^{\gamma} \quad (2)$$

where C is a constant and γ is the power factor. The plots of $\ln I_{ph}$ vs $\ln\phi$, are linear [**Figure 5(a)**] under different illuminations. From these curves γ is found to be less than unity. This sublinear dependence of I_{ph} on ϕ shows that photoconductivity in these thin films are of defect controlled type [28].

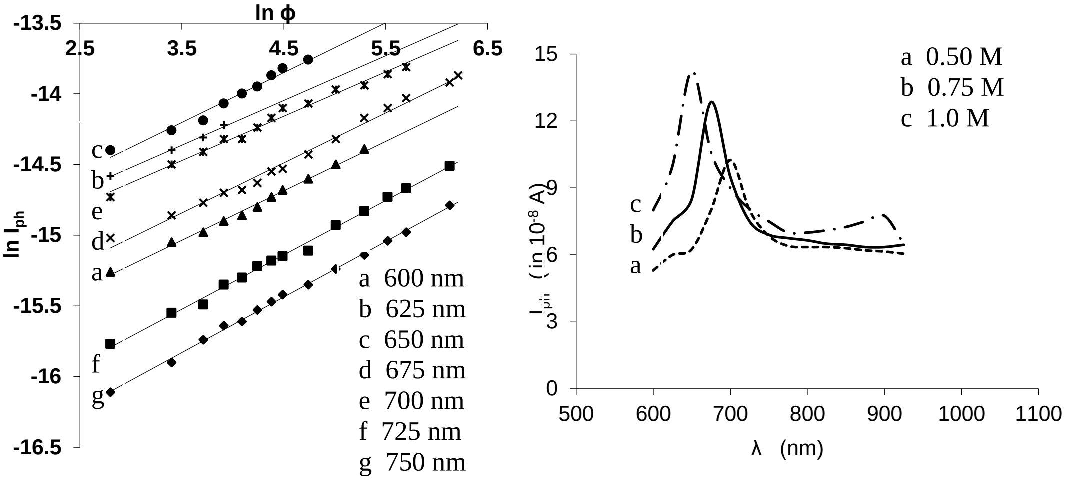

(a) (b)

Figure 5(a) lnI_{ph} vs lnϕ plot of a CdSe(t=240nm, m=1M) thin film under different monochromatic illuminations (b) Spectral response characteristics of nanocrystalline CdSe thin films of different m = 0.5, 0.75 and 1M.

Spectral response characteristics

In the vicinity of the absorption edge generally photoconductive materials show spectral distribution curve with more or less sharp peaks. From the plots of I_{ph} vs wavelength of monochromatic light(**Figure 5(b)**)it is seen that maximum absorption peak appears nearly in the wavelength range 650 to 700 nm, depending on various molarities of deposition, which corresponds to band gap values 1.90 to 1.77 eV respectively. This is more than that of the equivalent value for bulk CdSe (1.74 eV). The band gap increases with the increase in the molarity of deposition which is due to the nano phase formation in the thin films [24,29].The additional absorption peak which is being observed at around 875 nm along the longer side of wavelength of the 1M thin film is attributed to defects in the thin film [30]. The optical band gap corresponding to this lower peak is 1.41eV.Thus just by changing the molarity of the solution used for deposition of the thin films the band gaps of the deposited thin films may be altered. Such thin films are appropriate for application in different optoelectronic devices due to this band gap tunability property [1].

Temperature dependence of conductivity

The plots of lnσ vs 1,000/T for the thin films, both under dark and under illuminations show 2 conductivity regions (**Figure 6**), which means that in these thin films the conductivity σ cannot be represented by a single exponential form and the transport mechanism is characterized by a double activation process of the form.

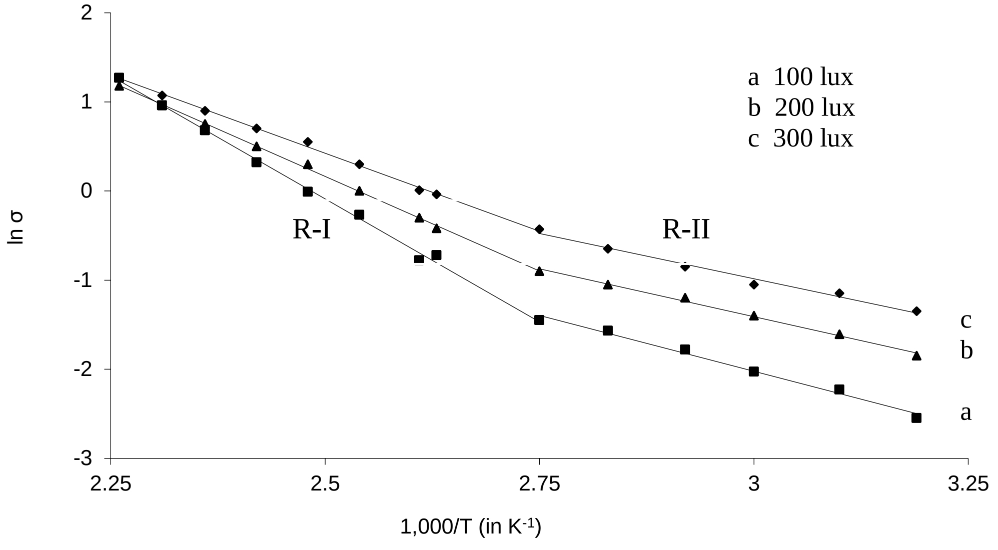

(a)

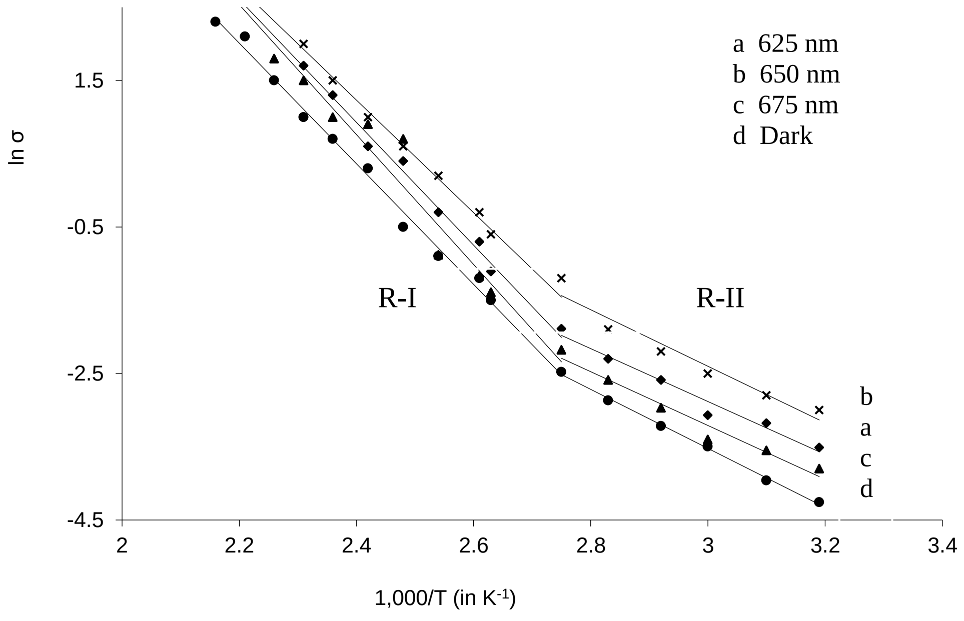

(b)

Figure 6 lnσ vs 1,000/T plot for a CdSe (t=240 nm, m=1M) thin film (a) under monochromatic light of 650 nm at different intensities (b) under dark and monochromatic illuminations of constant intensity.

$$\sigma = (\sigma_0)_1 \exp(-E_1/kT) + (\sigma_0)_2 \exp(-E_2/kT) \quad (3)$$

where E_1 and E_2 are the corresponding activation energies and the other symbols have their usual significance [31].

For the experimental thin film, the activation energies (E_a) are calculated from the slops of the lnσ vs 1,000/T plots whereas the mobility activation energies (E_{ma}) are calculated by subtracting the photo activation energies from the dark activation energies (**Table 1**). Similar types of results has also been reported by other workers [32-34]. For the thin film (t=240 nm, m=1M), grown at room temperature, the calculated values of E_a have been found to be 1.47 eV for high temperature region (R-I) and 0.87 eV for low temperature region (R-II).

Table 1 Calculated values of activation energies (E_a eV) amd mobility activation energies (E_{ma} eV) for a CdSe (t = 240 nm, m = 1 M) thin film (a) under different monochromatic illuminations of constant intensity (b) under monochromatic illumination of 650 nm of different intensities.

Wavelength	**650 nm**		**625 nm**		**675nm**	
Region	R-I	R-II	R-I	R-II	R-I	R-II
E_a	1.28	0.78	1.24	0.73	1.22	0.67
E_{ma}	0.49	0.39	0.53	0.34	0.55	0.50
Intensity	100 lux		200 lux		300 lux	
Region	R-I	R-II	R-I	R-II	R-I	R-II
E_a	1.24	0.73	1.19	0.68	1.16	0.62
E_{ma}	0.53	0.44	0.58	0.49	0.61	0.55

Growth and decay of photocurrent

The photocurrent at any instant of time during growth is given by the equation;

$$I_t = I_o\{1-\exp(1/ \tau_r)] \quad (4)$$

where I_o is the maximum photocurrent and τ_r is the growth time of photocurrent. With passage of time the photocurrent reaches a steady state and when the light is turned off the current decreases, because the excess number of carrier decreases as a result of rapid recombination. The decay may be represented by the equation;

$$I_t = I_o\{1-\exp (-t/\tau_d) \quad (5)$$

where t_d is the photocurrent decay time. It is observed that the experimental CdSe thin films exhibit a slow growth of photocurrent which is followed by an initial fast decay accompanied by a tail (**Figure 7**). The fast decay is associated with free electron-hole recombination and the subsequent region is due to release of electrons from traps.

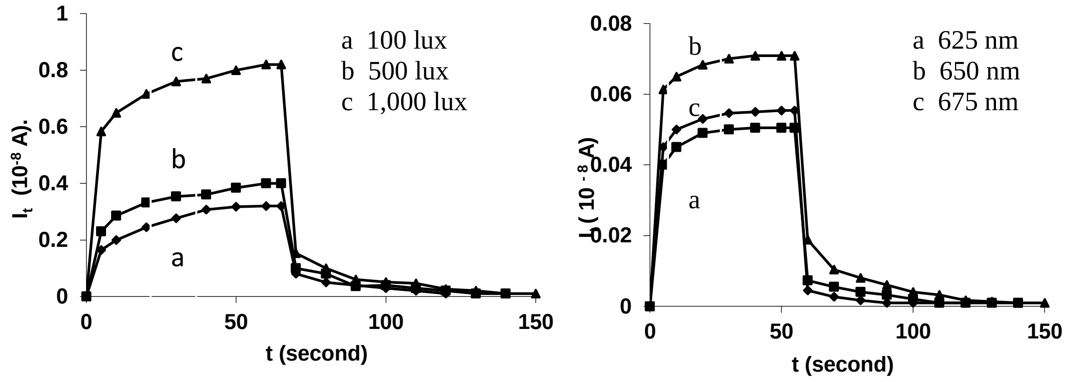

(a) (b)

Figure 7 Growth and decay of photocurrent for a CdSe (t=240 nm, m=1M) thin film (a) under monochromatic illumination of 650 nm of different intensities (b) under different monochromatic illuminations of constant intensity.

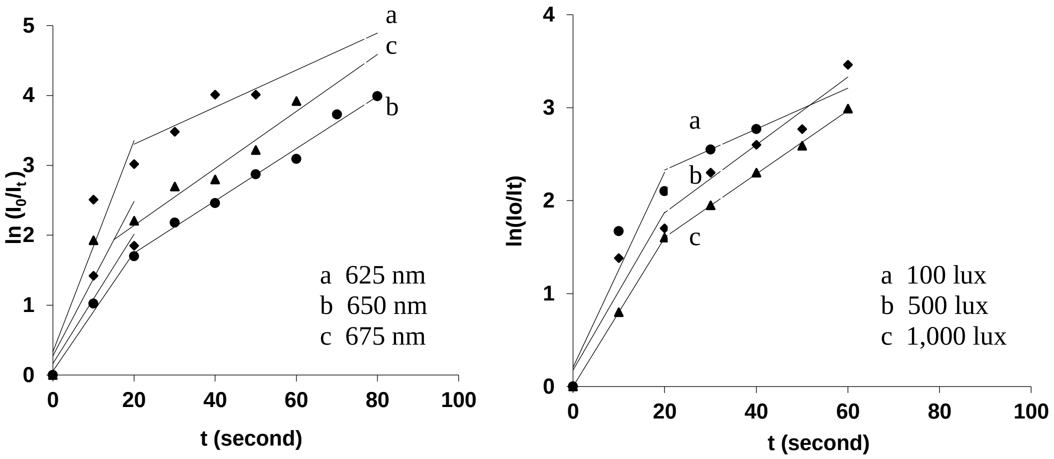

(a) (b)

Figure 8 ln(I_o/I_t) vs time t plot for a CdSe (t= 240 nm, m=1M) thin film (a) under different monochromatic illuminations of constant intensity (b) under monochromatic illumination of 650 nm of different intensities.

The trap depth E below the bottom of the conduction band or the top of the valenced band may be calculated using the simple decay law;

$$I_t = I_o\{1-\exp(-pt)\} \qquad (6)$$

where p is the probability of escape of an electron from the trap per second and is given by;

$$p = S \exp(-E/kT) \qquad (7)$$

Using these 2 relations, we get;

$$E = kT[\ln S - \ln\{\ln(I_o/I_t)/t\}] \qquad (8)$$

where T is the ambient temperature in K, I_o is the photocurrent at the instant of termination of illumination, I_t is the photocurrent at any instant of time t after termination of illumination, S is the frequency factor defined as the number per second that the quanta from the lattice vibrations attempt to eject the electron from trap, multiplied by the probability of transition of the ejected electron to the conduction band and is given by [35];

$$S=N_{eff}v_{th}S_t \qquad (9)$$

where N_{eff} is the effective density of states in the conduction band. It is assumed that at comparatively low temperature the number of occupied energy in the conduction band i.e. n is identical with N_{eff} [36], Now;

$$n = \sigma/e\mu \qquad (10)$$

where σ is the conductivity corresponding to photocurrent I_o. μ is the mobility of electrons in CdSe sample which is taken to be 580 cm^2V^{-1} s^{-1} [36];

S_t is the capture cross section of electron at temperature T and is given by;

$$S_t=\pi r^2 \qquad (11)$$

where r is radius of capture centre. It is calculated by putting coulomb energy of interaction of an electron with the corresponding trap which is equal to the thermal energy of the electron at temperature T [35]. i.e.

$$e^2/r\varepsilon = kT \tag{12}$$

$$\text{So; } S_t = \pi e^2/k^2T^2\varepsilon^2 \tag{13}$$

$$\text{At 300K; } S_t = 10^{-10}/\varepsilon^2 \text{ cm}^2 \tag{14}$$

where ε is the dielectric constant of CdSe sample which is taken to be 5.76 [37].

Table 2 Calculated values of trap depths for a CdSe (t= 240nm, m=1M) thin film (a) under different monochromatic illuminations of constant intensity 50 lux (b) under monochromatic illumination of 650nm of different intensities.

Illumination		σ (Ω cm)$^{-1}$ (in 10^{-5})	N_{eff} cm^{-3} (in 10^{10})	S Sec^{-1} (in 10^6)	E (eV)	
Intensity (lux)	Wavelength (nm)				E_1	E_2
50	650	0.71	6.51	4.66	0.59	0.62
	625	0.65	5.79	4.23	0.58	0.61
	675	0.73	6.65	4.75	0.61	0.63
100	650	0.60	5.3	3.91	0.58	0.61
500		0.69	6.38	4.62	0.60	0.62
1,000		0.97	8.51	5.83	0.61	0.62

The thermal velocity of an electron v_{th} is calculated by using the relation;

$$v_{th} = (2kT/m^*)^{1/2} \tag{15}$$

where m^* is the effective mass of an electron which is taken to be $0.13m_e$ [36].

For finding S, values of N_{eff}, v_{th} and S_t are separately calculated. Using the calculated values of S and p, evaluated from the slopes of $\ln(I_o/I_t)$ versus t plots (**Figure 8**), trap depths are calculated (**Table 2**) at different conditions of illuminations. From this figure it is observed that there exist 2 different slops in the plots, which indicates the existence of 2 distinct trap levels, E_1 and E_2, at the considered room temperature. The trap depths are not single valued and there is a quasi-continuous distribution of trap levels below the conduction band [21,34]. It may be noted that photocurrent in these thin films is found to obey a sub-linear relation with the intensity of illumination (**Figure 5(a)**) which may be explained on the basic of defect controlled photoconductivity mechanism.

Due to absorption of illuminating radiation free electron hole pairs are generated. The photogenerated electrons and holes which are in excess to the thermal equilibrium number density of carriers are responsible for the photoconduction process. One part of the photogenerated carriers recombine with respective opposite charges localized at grain boundary depletion region, thereby reducing the grain boundary potential barriers and the rest take part in the photoconduction process. As a result of reduction of this potential, the effective mobility of the carriers increases which brings the change in conductivity with intensity of illumination and this change is more towards the band edge wavelength. This process is known as barrier modulation [21].

Thus the increase of photoconductivity is due to 2 contributors viz one from resultant increase in the photogenerated carriers and other from the increase of effective mobility. Probably due to these phenomenon in case of the considered photoconducting nanocrystalline sample the usual relation that conductivityis inversely related to activation energy has not been found to be valid.

Although in this work data, for mainly one of the representative thin films are presented for the remaining thin films of other molarities, the basic nature of the different plots are more or less same, but for various thin films their response to the maximum photocurrent depends on wavelength of illumination which obviously brings a change to the numerical data.

Conclusions

CdSe thin films deposited at room temperature by CBD technique are of nanocrystalline nature and the optical band gaps of the films are easily tunable. Such thin films are found to be characterized by Poole-Frenkel type conductivity and barrier modulated photoconductivity. Photoconductivity of these thin films is basically controlled by the grain boundary defects. The photocurrent is dependent on the wavelength of excitation and increases towards the band edge wavelength. With the increase of intensity of incident monochromatic illumination activation energy decreases whereas mobility activation energy increases. But in case of wavelength of incident illumination these variations depends on the band edge wavelength. Rise and decay processes of photocurrent are effectively governed by different kind of traps. The trap depths have significant variation both with wavelength and intensity of incident illumination.

Acknowledgements

The authors acknowledge the University Grants Commission, India for funding Minor Research Project vide sanction letter no. F.5-206/2011-12/MRP/NERO/10829 for this work.

References

[1] PK Sahu, R Das and R Lalwani. Incorporation of tin in nanocrystalline CdSe thin films: A detailed study of optoelectronic and microstructural properties. *Appl. Phys. Mater. Sci. Process.* 2018; **124**, 665.

[2] S Hussain, M Iqbal, AA Khan, MN Khan, G Mehboob, S Ajmal, JM Ashfaq, G Mehboob, MS Ahmed, SN Khisro, CJ Li, R Chikwenze and S Ezugwu. Fabrication of nanostructured cadmium selenide thin films for optoelectronics applications. *Front. Chem.* 2021; **9**, 661723.

[3] NT Shelke, SC Karle and BR Karch. Photoresponse properties of CdSe thin film photodetector. *J. Mater. Sci. Mater. Electron.* 2020; **31**, 15061-9.

[4] PKSahu and R Das. Influence of trivalent bismuth doping on optoelectronic and microstructural properties of hydrophilic nanocrystalline cadmium selenide thin films. *Thin Solid Films* 2020; **693**, 137675.

[5] SA Gawali and CH Bhosale. Structural and optical properties of nanocrystalline CdSe and Al:CdSe thin films for photoelectrochemical application. *Mater Chem. Phys.* 2011; **129**, 751-5.

[6] D Nesheva, Z Aneva, S Reynolds, C Main and AG Fitzgerald. Preparation of micro and nanocrystalline CdSe and CdS thin films suitable for sensor applications. *J. Optoelectron. Adv. Mater.* 2006; **8**, 2120-5.

[7] WS Lee, YG Kang, HK Woo, J Ahn, H Kim, D Kim, S Jeon, MJ Han, J Choi and SJ Oh. Designing high-performance CdSe nanocrystal thin-film transistors based on solution process of simultaneous ligand exchange, trap passivation, and doping. *Chem. Mater.* 2019; **31**, 9389-99.

[8] S Nizamoglu, T Ozel, E Sari and HV Demir. White light generation using CdSe/ZnS core-shell nanocrystals hybridized with InGaN/GaN light emitting diodes. *Nanotechonology* 2007; **18**, 065709.

[9] S Mathuri, K Ramamurthi and RR Babu. Effect of Sb incorporation on the structural, optical, morphological and electrical properties of CdSe thin films deposited by electron beam evaporation technique. *Thin Solid Films* 2018; **660**, 23-30.

[10] HN Rosly, KS Rahman, MN Harifand and C Doroody. Annealing temperature assisted microstructural and optoelectrical properties of CdSe thin film grown by RF magnetron sputtering. *Superlattice. Microst.* 2020; **148**, 106716.

[11] Y Yang, T Guo, D Wang, X Xiong and B Li. Preparation and characterization of pulsed laser deposited CdSe window layer for Sb2Se3 thin film solar cell. *J. Mater. Sci. Mater. Electron.* 2020; **31**, 13947-56.

[12] W Pan, J Liu, Z Zhang, R Gu, A Suvorova, S Gain, H Wang, Z Li, L Fu, L Faraone and W Lei. Large area van der Waals epitaxy for II-VI CdSe thin films for flexible optoelectronics and full-color imaging. *Nano Res.* 2022; **15**, 368-76.

[13] M Hassen, R Riahi, F Laatar and H Ezzaouia. Optical and surface properties of CdSe thin films prepared by sol-gel spin coating method. *Surface. Interfac.* 2020; **18**, 100408.

[14] RC houdhary and RP Chauhan. Nitrogen ion implantation effects on the structural, optical and electrical properties of CdSe thin film. *J. Mater. Sci. Mater. Electron.* 2018; **25**, 12595-602.

[15] MS Deora and SK Sharma. Effect of incorporation of sulphur on the structural, morphological and optical studies of CdSe thin films deposited by solution processed spin coating technique. *Thin Solid Films* 2019; **670**, 68-75.

[16] A Alasvand and H Kafashan. Comprehensive physical studies on nanostructured Zn doped CdSe thin films. *J. Alloy. Comp.* 2019; **789**, 108-18.

[17] AM Abdulwahab, AA AL-Adhreai and AAA Ahmed. Influence of Ni-Co dual doping on structural and optical properties of CdSe thin films prepared by chemical bath deposition method. *Optik* 2021; **236**, 166659.

[18] PK Sahu, R Das and R Lalwani. Preparation of nanocrystalline Mg doped CdSe thin films and their optical, photoluminescence, electrical and structural characterization. *J. Mater. Sci. Mater. Electron.* 2017; **28**, 18296-306.

[19] AG Habte, FG Hone and FB Dejene. The influence of malonic acid on the structural, morphological and optical properties of CdSe thin films prepared by chemical bath deposition method. *Inorg. Chem. Comm.* 2019; **103**, 107-12.

[20] SK Tripathi, AS Al-Kabbi, K Sharma and GSS Saini. Mobility lifetime product in doped and undoped nanocrystalline CdSe. *Thin Solid Films* 2013; **548**, 406-10.

[21] K Sarmah and R Sarma. Mobility activation in thermally deposited CdSe thin films. *Bull. Mater. Sci.* 2009; **32**, 369-73.

[22] K Sarmah, R Sarma and HL Das. Effect of wavelength and intensity of illumination on the photoelectronic properties of CdSe thin films. *Indian J. Phys.* 2008; **82**, 585-94.

[23] MN Borah, BJ Baruah, S Chaliha, DP Gogoi, U Mcfarlane and S Dutta. Structural analysis of chemically deposited nanocrystalline CdSe films. *J. Exp. Nanosci.* 2012; **8**, 1-7.

[24] MN Borah and S Chaliha. Characterization of chemically deposited nanocrystalline CdSe thin films from transmittance spectra. *Mater. Today Proc.* 2021; **46**, 5777-80.

[25] LI Maissel and R Glang. *Hand book of thin film technology*. McGraw Hill Book, New York, 1970.

[26] Joint Committee on Powder Diffraction Standards. Set 20 powder diffraction file. *Anal. Chem.* 1970; **42**, 81A.

[27] A Goswami. *Thin film fundamentals*. New Age International, New Delhi, 1996.

[28] R Devi, P Purkayastha, PK Kalita, R Sarma, HL Das and BK Sarma. Photoelectric properties of CdS thin film prepared by chemical bath deposition. *Indian J. Pure Appl. Phys.* 2007; **45**, 624-7.

[29] MK Khalaf, BAM ALhilli, AI Khudiar and AA Alzahra. Influence of nanocrystalline size on optical band gap in CdSe thin films prepared by DC sputtering. *Photon. Nanostructures Fund. Appl.* 2016; **18**, 59-66.

[30] R Devi, P Purkayastha, PK Kalita and BK Sarma. Synthesis of nanocrystalline CdS thin films in PVA matrix. *Bull. Mater. Sci.* 2007; **30**, 123-8.

[31] C Mehta, JM Abbas, GSS Saini and SK Tripathi. Electrical and optical properties of n-CdSe. *J. Optoelectronics Adv. Mater.* 2008; **10**, 2461-5.

[32] RB Kale, SD Sartale, BK Chougule and CD Lokhande. Growth and characterization of nanocrystalline CdSe thin films deposited by the successive ionic layer adsorption and reaction method. *Semicond. Sci. Tech.* 2004; **19**, 980-6.

[33] PP Hankare, SD Delekar, PA Chate, SD Sabane, KM Garadkar and VM Bhuse. A novel route to synthesize $Cd_{1-x}Pb_{x}Se$ thin films from solution phase. *Semicond. Sci. Tech*. 2005; **20**, 257-64.

[34] J Sharma, R Singh, A Kumar, T Singh, P Agrawal and A Thakur. Size-controlled synthesis of nanocrystalline CdSe thin films by inert gas condensation. *Appl. Nanosci.* 2018; **8**, 359-67.

[35] RH Bube. *Photoconductivity in solids*. John Wiley and Sons,New York, 1960.

[36] SS Devlin. *Physics and chemistry of II-VI compounds*. *In*: M Aven and J Prener (Eds.). North Holand Publishing Company, Amsterdam, Netherlands, 1967.

[37] PK Kalita, BK Sarma and HL Das. Space charge limited conduction in CdSe thin films. *Bull. Mater Sci*. 2003, **26**, 613-7.